Toxicology Reports 10 (2023) 529–536

Contents lists available at ScienceDirect

Toxicology Reports

journal homepage: www.elsevier.com/locate/toxrep

Zinc oxide nanoparticles trigger autophagy-mediated cell death through activating lysosomal TRPML1 in normal kidney cells

Boyun Kim [a], Gaeun Kim [a,c], Soyeon Jeon [b], Wan-Seob Cho [b], Hyun Pyo Jeon [a,c,*], Jewon Jung [a,c,*]

[a] Department of SmartBio, College of Life and Health Science, Kyungsung University, Busan, the Republic of Korea
[b] Department of Health Sciences, The Graduate School of Dong-A University, Busan, the Republic of Korea
[c] Graduate School of Chemical Safety Management, Kyungsung University, Busan, the Republic of Korea

ARTICLE INFO

Handling Editor: Dr. L.H. Lash

Keywords:
Zinc oxide nanoparticles
Autophagy
Lysosome
TRPML1
Kidney

ABSTRACT

Zinc oxide nanoparticles (ZnO NPs) have been widely used in various materials including sunscreens, cosmetics, over-the-counter topical skin products, and pigments. As traces of the used ZnO NPs have been found in the kidney, it is crucial to uncover their potential risks. The aim of this study is to elucidate detrimental effects of ZnO NPs and the molecular mechanism behind their renal toxicity. Cytotoxic effects were measured by MTT assay after HK2 cells were exposed to ZnO NPs for 24 h and IC_{50} value was determined. ROS and intracellular Zn^{2+} levels were detected by flow cytometry, and localization of Zn^{2+} and lysosome was determined by confocal microscopy. Occurrence of autophagy and detection of autophagic flux were determined by Western blot and confocal microscopy, respectively. We performed unpaired student *t* test for two groups, and one-way ANOVA with Tukey's post hoc for over three groups. ZnO NPs induced cell death in human renal proximal tubule epithelial cells, HK2. Cytosolic Zn^{2+} caused autophagy-mediated cell death rather than apoptosis. Cytosolic Zn^{2+} processed in lysosome was released by TRPML1, and inhibition of TRPML1 significantly decreased autophagic flux and cell death. The findings of this study suggest that ZnO NPs strongly induce autophagy-mediated cell death in human kidney cells. Controlling TRPML1 can be potentially used to prevent the kidney from ZnO NPs-induced toxicity.

1. Introduction

Zinc oxide nanoparticles (ZnO NPs) are widely and increasingly used in multiple applications including agriculture, food, and cosmetics, due to their electrical and optical properties [1]. More recently, ZnO NPs are utilized in the biomedical and pharmaceutical field, such as drug delivery and imaging system [2,3]. Given the widespread use of ZnO NPs, it is crucial to pay attention to their potential risks, including cytotoxicity, genotoxicity, and inflammatory effects [4]. Previous studies have reported that oral administration of ZnO NPs induces hepatotoxicity in mice and renal toxicity in rats through oxidative stress [5,6]. However, the underlying mechanism of cellular toxicity is still unclear.

Zn^{2+} is an essential ionic signaling molecule that regulates protein functions by interacting with sulfur of cysteine in cellular proteins and affects multiple cellular processes including enzymatic activity, gene expression, and signal transduction [7,8]. However, the excessive Zn^{2+} such as by entering ZnO NPs can disrupt cellular Zn^{2+} homeostasis, leading to cell death via mitochondrial damage and pathologies such as growth defects, immune dysfunction, and neurodegenerative diseases [9–11]. If NPs including ZnO NPs enter the body, they circulate in the bloodstream, and mainly accumulate in the liver, spleen, heart, and kidney [12,13]. Since urinary excretion of ZnO NPs is one of the available routes to clear out Zn^{2+}, the renal hazards of ZnO NPs should be investigated.

At the cellular level, extracellular NPs are internalized by endocytosis and transported into lysosomes where NPs are processed [14]. In case of ZnO NPs, dissipation of lysosomal Zn^{2+} processed from ZnO NPs into the cytosol is at least in part regulated by transient receptor potential mucolipin 1 (TRPML1) [15]. TRPML1 is a Ca^{2+} and Zn^{2+} cation channel localized in late endosome and lysosome [16,17]. The

Abbreviations: ZnO NPs, Zinc Oxide Nanoparticles; TRPML1, Transient receptor potential mucolipin 1.

* Correspondence to: Department of SmartBio, College of Life and Health Science, Kyungsung University, 309 Suyeong-ro Room 507-2, Nam-gu, Busan 48434, the Republic of Korea.
E-mail addresses: hpjeon@ks.ac.kr (H.P. Jeon), jewonjung@ks.ac.kr (J. Jung).

https://doi.org/10.1016/j.toxrep.2023.04.012
Received 14 January 2023; Received in revised form 14 April 2023; Accepted 24 April 2023
Available online 25 April 2023

accumulating evidence suggests TRPML1 plays an essential role in regulation of endocytosis and exocytosis, lysosomal adaptation to nutrient starvation, and induction of autophagy [18–20]. Additionally, oxidative stress activates TRPML1 and subsequently Ca^{2+} are released from the lumen into the cytosol, which leads to enhance autophagy [21, 22]. According to recent identification, cell death in metastatic melanoma is mediated by lysosomal Zn^{2+} irrespective of the apoptotic pathway [23]. In the present study, we demonstrated TRPML1 releases Zn^{2+} processed from ZnO NPs in lysosome and the released Zn^{2+} triggers autophagy-mediated cell death in human kidney cells. We also found that pharmacologic inhibition of TRPML1 interrupts the efflux of Zn^{2+} to cytosol, leading to protect renal cells from ZnO NPs-induced cell death.

2. Materials and methods

2.1. Reagents

Zinc Oxide nanoparticles (ZnO NPs) purchased from Sigma-Aldrich (MO, USA) were suspended in phosphate-buffered saline (PBS) and ultrasonicated for 5 min to avoid aggregation before treating to the cells. The ZnO NPs were reconstituted in the culture medium with serial concentrations. ZnO NPs, ML-SI1 (also known as GW405833), N-acetyl-L-cysteine (NAC), 2,7-Dichlorofluorescein (DCF), 3-Methyladenine (3-MA), Diethylenetriaminepentaacetic acid (DTPA), and N,N,N′,N′-Tetrakis(2-pyridylmethyl)ethylenediamine (TPEN) were purchased from Sigma-Aldrich. Bafilomycin A1 was obtained from TOCRIS (Bristol, United Kingdom). LysoTracker Red DND-99 and FluoZin™-3, AM, and FITC Annexin V/Dead Cell Apoptosis kit were purchased from Thermo Fisher Scientific (CA, USA).

2.2. Characterization of ZnO NPs

The primary size and distribution of ZnO NPs were determined by transmission electron microscopy (TEM; JEM-1200EX II, JEOL, Tokyo, Japan). The hydrodynamic size and zeta potential in culture medium containing 10% fetal bovine serum (FBS) were measured by a Zetasizer Nano ZS (Malvern, Malvern Hills, UK).

2.3. Cell culture

HK2 cells purchased from Korean Cell Line Bank (Korea) were cultured in RPMI-1640 (Welgene, Korea) containing 4.5 g/L D-glucose, 2 mM L-glutamine, 10 mM HEPES, 1 mM sodium pyruvate, 1.5 g/L sodium bicarbonate, 10 % FBS (Gibco), 100 U/ml penicillin, and 100 g/ml streptomycin (Gibco). The cultured cells were maintained at 37 °C in a humidified atmosphere of 5 % CO_2.

2.4. Cytotoxicity Assay

To determine cell viability following treatment of ZnO NPs, 3-(4,5-dimethylthiazol-2-yl)-2,5-diphenyltetrazolium bromide (MTT) assay was conducted. HK2 cells following exposure to ZnO NPs for 24 h were incubated with 2 mg/ml MTT at 37 °C for 3 h in the dark. Afterwards, dimethyl sulfoxide (DMSO) was added to dissolve formazan transformed by live cells. Absorbance was measured at 540 nm by a microplate reader (SpectraMax® ABS, Molecular Devices).

2.5. Quantitative Real Time Polymerase Chain Reaction (qRT-PCR)

A total RNA was extracted from HK2 cells cultured in presence of vehicle (PBS) or 20 μg/ml of ZnO NPs using TRIzol reagent (Ambion, Life Technologies) according to the manufacturer's instructions. Reverse transcription was carried out with 500 ng of total RNA using a High-Capacity cDNA RT kit (Applied Biosystems, Thermo Fisher Scientific) on a Bio-Rad T100 thermal cycler (Bio-Rad). SYBR green-based qRT-PCR was performed on a QuantStudio™ 3 Real-Time PCR System (Applied Biosystems) to analyze expression of target genes, including *MCOLN1*, *HO1*, *NRF2*, *SOD2*, and *TRX* (Primer sequences are in Table S1). The relative abundance of mRNA was normalized reference gene, GAPDH. All primers were purchased from Macrogen (Korea).

2.6. Western blotting

HK2 cells were harvested following treatment of vehicle or ZnO NPs and lysed with RIPA buffer containing 20 mM Tris-HCl pH 8.0, 150 mM NaCl, 1 mM EDTA, 1 % Triton X-100, 0.1 % sodium deoxycholate, 1 mM phenylmethylsulfonyl fluoride (PMSF), 1 mM sodium orthovanadate (Na_3VO_4), and 1 × protease inhibitor cocktail. Lysates were centrifuged at 12,000 × *g* at 4 °C for 15 min and supernatant (whole protein) was transferred to new tubes. The extracted protein was quantified using a Pierce BCA protein assay kit (Thermo Scientific). A total 10–20 μg of protein per well was separated using 8–15 % SDS-PAGE, and then transferred to 0.45 μm poly-vinylidene fluoride (PVDF) membrane (Bio-Rad). After blocking with 5 % skim milk solution in Tris-buffered saline with 0.1 % Tween-20, the membrane was probed with antibodies including caspase 3, caspase 7, LC3, p62, Actin (Cell signaling technology), and TRPML1 (Abcam). Signals were visualized using a chemiluminescence detection kit.

2.7. Measurement of Reactive Oxygen Species (ROS)

DCF was utilized to measure ROS response to treatment of ZnO NPs in HK2 cells. After exposure to 20 μg/ml of ZnO NPs, HK2 cells were incubated with 2.5 μM of DCF at 37 °C for 30 min in the dark. Relative fluorescence intensity of DCF was quantified by a BD FACS™ Universal Loader (BD Biosciences).

2.8. Measurement of intracellular Zn^{2+} level

FluoZin™-3, AM was utilized to detect intracellular Zn^{2+}. HK2 cells exposed to ZnO NPs for 24 h were incubated with 100 nM FluoZin™-3, AM at 37 °C for 30 min in the dark. Relative fluorescence intensity of FluoZin-3 was detected and quantified by a BD FACS™ Universal Loader.

2.9. Confocal microscopy

To observe localization of intracellular Zn^{2+} and lysosome following exposure to ZnO NPs for 24 h, HK2 cells were incubated with 100 nM of LysoTracker Red DND-99 at 37 °C for 1 h and then stained with 100 nM FluoZin™-3, AM at 37 °C for 1 h in the dark. The cells were washed twice with PBS. The visualization was performed by a Nikon AX confocal microscope (Nikon, Japan). To measure autophagic flux altered by ZnO NPs, 2 μg of GFP-LC3-RFP plasmid were transfected to HK2 cells using lipofectamine™ 2000 reagent according to the product manual (Thermo Fisher Scientific). The fluorescent signal was detected by the Nikon AX confocal microscope (Nikon, Japan).

2.10. Knock-down using siRNA against MCOLN1

HK2 cells were transfected with 4 different sets of siRNA duplexes against *MCOLN1* (Table S2; Bioneer, Korea) and siRNA universal negative control #1 (Sigma Aldrich). At 48 h of post-transfection, cells were exposed to ZnO NPs for 24 h, and then used for further experiments, including Western blotting, MTT assay, and immunofluorescence.

2.11. Statistical analysis

Data were analyzed using GraphPad Prism 9 (San Diego, CA) and presented as mean ± standard error of mean (SEM) of at least three independent experiments. Normal distribution was evaluated with Shapiro-Wilk test. For normally distributed data, we performed the

unpaired *t* test for comparing two groups and one-way analysis of variance (ANOVA) for comparing three or more than three categorical groups. Significant difference following one-way ANOVA was determined by Tukey's test for post hoc analysis.

3. Results

3.1. ZnO NPs cause cell death in human kidney epithelial cells via generation of Zn^{2+}

The characterization of ZnO NPs used in the present study was determined by TEM. The particles had a mixture of rod and spherical shapes in their morphology (Fig. 1A) and primary size was 110.98 ± 58.29 nm (Fig. 1B). The zeta potential of ZnO NPs was − 10.3 ± 0.3 mV, and hydrodynamic size with dynamic light scattering (DLS) was 288.8 ± 21.7 nm in culture medium supplemented with 10 % FBS (Fig. 1C).

As damages in renal tubular epithelial cells play a role in the pathological process of both acute and chronic kidney diseases, we chose a human renal proximal tubule epithelial cell line, HK2. To identify the cytotoxic effect of ZnO NPs on HK2 cells, serial concentrations of ZnO NPs were exposed for 24 h. ZnO NPs were sonicated for 5 min to homogenize the particles to prevent from aggregation, before treating ZnO NPs in every experiment. Treatment of ZnO NPs caused the decrease of cell viability at 24 h, and IC_{50} value of ZnO NPs was approximately 20 μg/mL (Fig. 2A). In the further experiments, we treated 20 μg/mL of ZnO NPs based on IC_{50} value. Since ZnO NPs are rapidly dissolved into Zn^{2+}, we detected free intracellular Zn^{2+} using FluoZin-3 AM following treatment of ZnO NPs. Treatment of ZnO NPs generated a significant amount of Zn^{2+} (Fig. 2B), and subsequently reduced cell viability (Fig. 2C). To clarify whether generation of intracellular Zn^{2+} contributes to cell death, Zn^{2+}-chelator, diethylenetriamine pentaacetate (DTPA), was added to ZnO NP-treated HK2 cells. DTPA treatment significantly blocked intracellular Zn^{2+} generation (Fig. 2B), and allowed to recover cell viability as much as vehicle-treated group (Fig. 2C). To confirm whether cell death is dependent on caspase activity, we examined cleavage of executioner caspase 3 and 7 by treatment of ZnO NPs. Interestingly, ZnO NPs completely inhibited the cleavage of caspase 3 and 7 (Fig. 2D and S5). To ensure that the observed cell death was not due to apoptosis, we performed Annexin V (green) and PI (red) staining. As shown in Fig. 2E, there were fewer Annexin V-positive cells in the ZnO NPs-treated cells compared to cisplatin (CDDP)-treated cells (positive control), indicating that the cell death induced by ZnO NPs was not primarily due to apoptosis. Collectively, these data suggest that cytosolic Zn^{2+} released from ZnO NPs mediates HK2 cell death, but not via caspase-dependent apoptotic pathways.

3.2. ZnO NPs induce autophagy-dependent cell death rather than apoptosis

Since ZnO NP-induced cell death was independent of the caspase activity, it was necessary to verify that ZnO NPs-induced cell death mediates autophagy. As our expectation, the exposure to ZnO NPs induced lipidation of LC3 and increased p62 expression. Torin1 (mTOR inhibitor) was used as a positive control (Fig. S1A, S1B, and S6). Both LC3 lipidation (LC3-II) and p62 expression were alleviated by DTPA treatment (Fig. 3A, 3B, and S7), which means generation of intracellular Zn^{2+} is associated with autophagic flux. TPEN (another Zn^{2+} chelator) was also alleviated LC3 lipidation and p62 expression (Fig. 3C, 3D, and S8). Similar to the results observed with DTPA (shown in Fig. 2C), TPEN treatment partially protected cells against ZnO-induced cell death (Fig. 3E). Bafilomycin A1 (BafA1) is an inhibitor of autolysosome, which blocks the fusion of autophagosome and lysosome. To confirm whether blocking autophagic flux protects against cell death caused by the increase of intracellular Zn^{2+}, we measured intracellular Zn^{2+} using FluoZin-3 AM following treatment with BafA1. BafA1 significantly interrupted the generation of intracellular Zn^{2+} generation (Fig. 3F) and partially allowed to recover cell viability (Fig. 3G). Interrupting the formation of ZnO-mediated autolysosomes was confirmed by the accumulation of LC3 lipidation and p62 in BafA1-treated cells, which means BafA1 hinders autophagic clearance (Figs. 3H, 3I, and S9). Similarly, the inhibition of autophagosome formation using 3-MA decreased ZnO-mediated LC3 lipidation (Fig. S2A, S2B, and S10), and partially protected from autophagic cell death (Fig. S2C). A fluorescent probe GFP-LC3-RFP was introduced to HK2 cells to evaluate autophagic flux. The autophagic flux can be measured by calculating the ratio of GFP to RFP. If the merged color is yellow, it indicates low autophagic flux. If the merged color is red, it indicates high autophagic flux [24]. When HK2 were exposed to ZnO NPs for 24 h, the intensity of GFP was diminished and the merged color of RFP and GFP signals was closer to red compared to vehicle-treated cells, indicating GFP-LC3 was degraded by autolysosome (Fig. 3J). Taken together, these findings suggest that ZnO NPs encourage autophagy-mediated cell death in HK2.

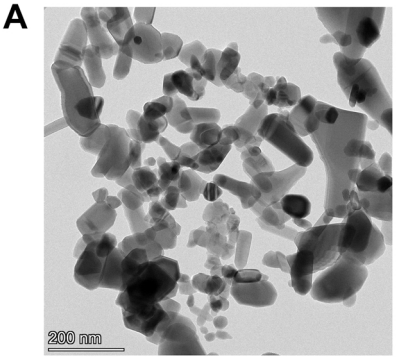

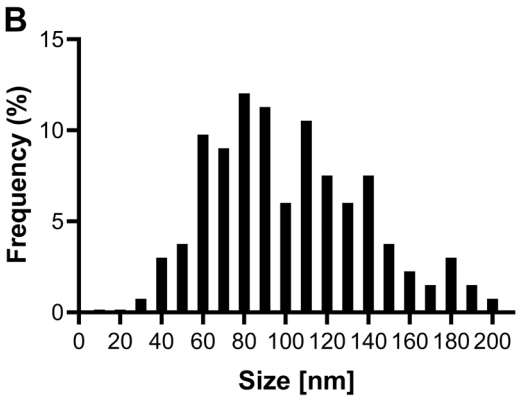

C

	Hydrodynamic diameter (nm)	PDI	Zeta potential (mV)
ZnO	288.8	0.165	-10.3

Fig. 1. Characterization of ZnO NPs used in the present study. (A, B) Structural characterization and particle size distribution of ZnO NPs were obtained by TEM. (C) Hydrodynamic size and zeta potential of ZnO NPs were measured in complete culture medium containing 10 % FBS.

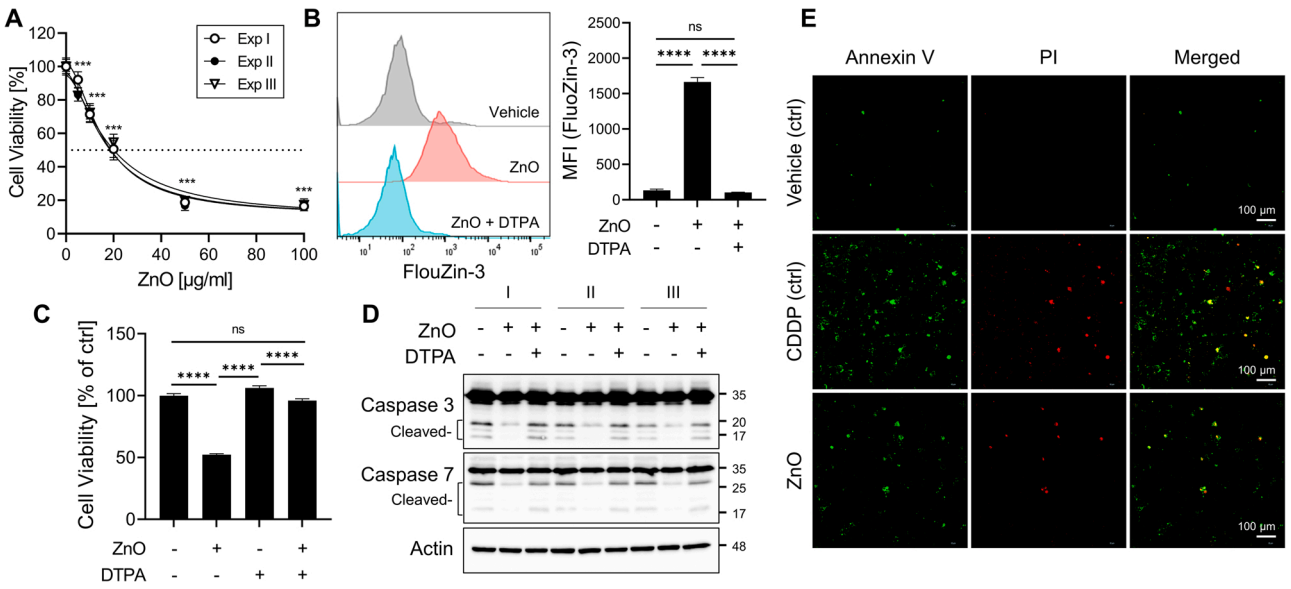

Fig. 2. Zn^{2+} generated from ZnO NPs induces cell death in proximal tubule epithelial cells. (A) HK2 cells were exposed to serial concentrations of ZnO NPs for 24 h. ZnO NP-induced cytotoxicity was determined by MTT assay. IC_{50} value was calculated by GraphPad Prism 9. (B) Intracellular Zn^{2+} level was measured and quantified by flow cytometry. (C) After treatment of 20 μg/ml ZnO NPs and 1 mM DTPA, cell viability was determined by MTT assay. (D) Western blot image shows activities of caspase 3 and caspase 7. Actin was used as an internal control. (E) Annexin V and PI staining indicates ZnO NP-induced apoptosis in HK2 cells. Cisplatin (CDDP) was used for positive control. All data are represented as mean ± SEM. ****$p < 0.0001$.

3.3. Lysosomal TRPML1 mediates to generate cytosolic Zn^{2+} with cytotoxicity

Exposure to NPs including ZnO NPs or damages in cellular organelle induce oxidative stress, resulting in cytotoxicity [25,26]. In order to confirm the relevance of ROS in our study, ROS generation was determined by detection of DCF using flow cytometry. We observed ZnO NPs significantly increased intracellular ROS level (Fig. S3A). Chelating Zn^{2+} using DTPA blocked to generate ROS as much as NAC-treated group. Scavenging ROS with NAC partially protected from cell death caused by ZnO NPs (Fig. S3B). Additionally, antioxidant genes including *HO1*, *NRF2*, *SOD2*, and *TRX* were highly expressed in response to treatment of ZnO NPs (Fig. S3C). According to a paper published in 2016, high level of ROS directly and specifically activates TRPML1 that regulates the release of cation from lysosome [22,23]. Based on the previous study, we investigated the relevance of TRPML1 with Zn^{2+}-mediated cell death. Treatment of ZnO NPs enhanced gene (*MCOLN1*) and protein expression of TRPML1 in 24 h (Fig. 4A–C, and S11). The exposure to ZnO NPs increased cytosolic Zn^{2+} level compared to vehicle-treated cells (Fig. 4D). Inhibition of TRPML1 by ML-SI1 did not alter the total intracellular Zn^{2+} level (Fig. 4D). However, ML-SI1 facilitated the localization of Zn^{2+} to lysosomes, leading to the decrease of cytotoxic cytoplasmic Zn^{2+} level by blocking the efflux of Zn^{2+} from lysosome to the cytoplasm (Fig. 4E). To further confirm the role of TRPML1 inhibition, we depleted endogenous TRPML1 by treatment with specific siRNAs. The two duplexes of siRNA against *MCOLN1* (#3 and #4) were found to reduce TRPML1 expression (Fig. 4F, and S12). Depletion of TRPML1 using siRNA #3 facilitated the localization of Zn^{2+} to lysosomes (Fig. 4G), resulting in the decreased cytoplasmic Zn^{2+} level that led to increased cell viability (Fig. 4H). In contrast, negative control siRNA-treated cells exhibited high levels of cytoplasmic Zn^{2+} (Fig. 4G). Furthermore, the scavenging of ROS using 10 mM NAC led to the localization of Zn^{2+} to lysosomes and a reduction in cytoplasmic Zn^{2+} level, indicating NAC probably blocks the release of lysosomal Zn^{2+} through TRPML1 (Fig. S4). These findings propose that ZnO NP-induced ROS probably activate TRPML1, which are responsible for the excessive level of cytosolic Zn^{2+}.

3.4. Inhibition of TRPML1 blocks autophagic flux caused by ZnO NPs in HK2

To figure out that TRPML1 activity influences autophagic flux, we transfected GFP-LC3-RFP plasmid to HK2 cells and then ZnO NPs were treated for 24 h. Pharmacologic inhibition of TRPML1 (close to yellow) activity by ML-SI1 showed a strong intensity of GFP compared to ZnO NPs-treated cells (close to red due to weak signal of GFP; Fig. 5A), which means that inhibition of TRPML1 mitigated to create autolysosome. In addition, ML-SI1 partially alleviated autophagy-mediated cell death (Fig. 5B). Collectively, TRPML1 inhibition attenuated autophagic flux from autophagosome to autolysosome, resulting in cell protection from ZnO NPs.

4. Discussion

The present study aimed to investigate the mechanism underlying the cytotoxicity of ZnO NPs on human renal tubule epithelial cells. We identified ZnO NPs significantly caused cell death in 24 h of exposure. Since the cell death was not mediated by activation of executioner caspases, we investigated ZnO NP-induced autophagy as a cell death mechanism. In response to ZnO NP treatment, LC3 lipidation was significantly elevated, which coincided with the increase of autophagic flux. Inhibition of autophagic flux using BafA1 and 3-MA significantly alleviated cytotoxicity caused by ZnO NPs. When ZnO NPs were exposed to HK2 cells, cytosolic Zn^{2+} and intracellular ROS levels were increased. Both Zn^{2+} chelator and ROS scavenger inhibited the increase of cytosolic Zn^{2+} and subsequently protected from cell death. Furthermore, ZnO NPs induced TRPML1 gene (*MCOLN1*) and protein expression, which means ZnO NP can activate TRPML1 and release Zn^{2+} from lysosome to cytoplasm. Pharmacologic inhibition of TRPML1 using ML-SI1 and genetic inhibition using siRNA against *MCOLN1* interrupted the dissipation of lysosomal Zn^{2+} to the cytoplasm and blocked autophagic flux. Subsequently, ZnO NP-induced autophagic cell death was alleviated.

Our findings that cleavage of both caspase 3 and 7 was totally inhibited by treatment of ZnO NPs are alignment with previously investigated studies [27,28]. It has been reported that micromolar concentrations of Zn^{2+} significantly mitigated apoptotic process and

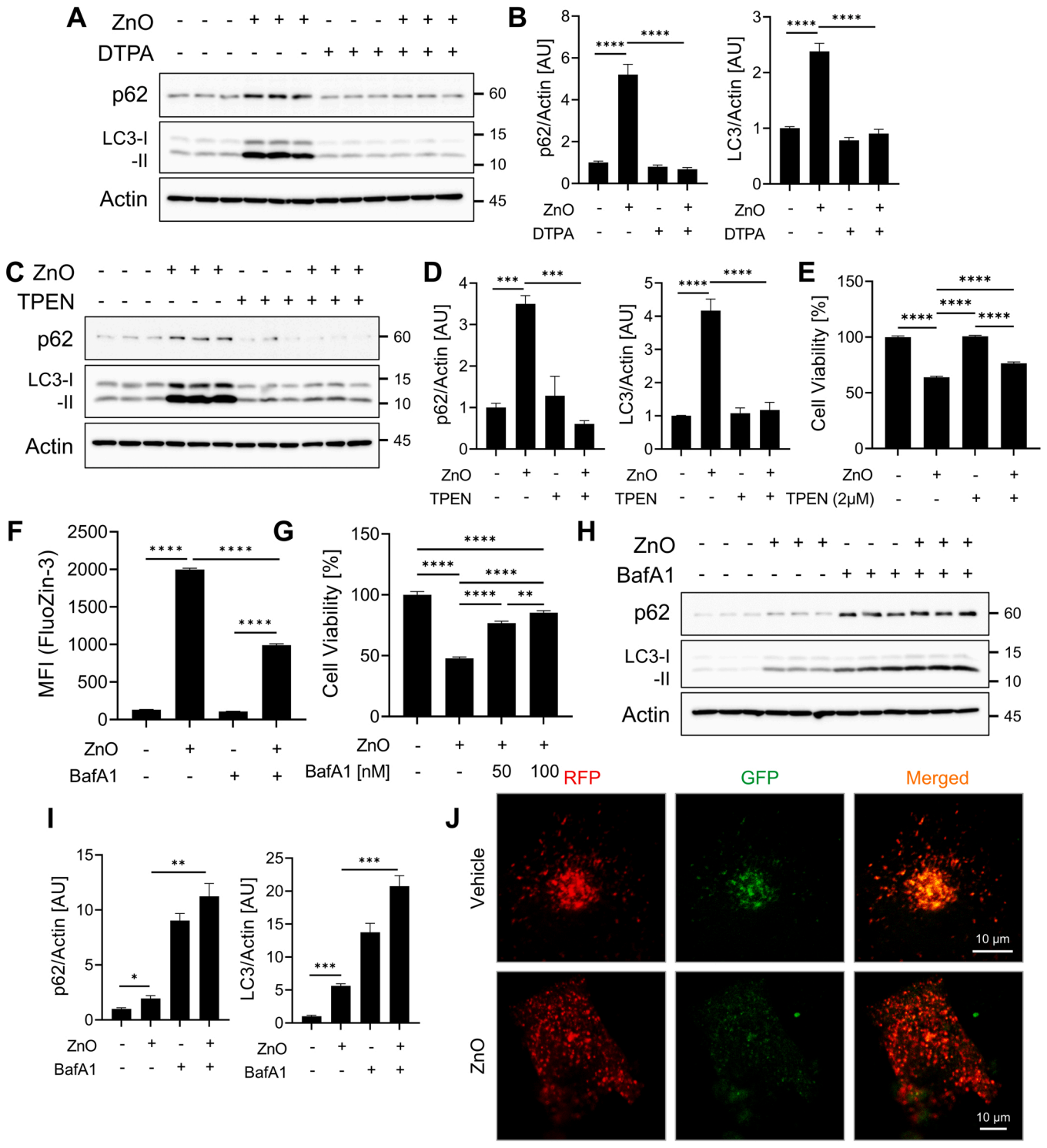

Fig. 3. ZnO NPs encourage autophagy-mediated cell death in HK2. (A) Western blot data indicate LC3 lipidation (LC3 II) and p62 expression induced by ZnO NPs. (B) Western blot bands were quantified using Image J (AU: arbitrary unit). (C) Western blot images indicate TPEN treatment alleviates LC3 lipidation and p62 expression. (D) Western blot bands were quantified using Image J (AU: arbitrary unit) (E) Cell viability recovered by TPEN was determined by MTT assay. (F) After treating ZnO NPs and 100 nM BafA1 for 24 h, the cells were stained with FluoZin-3 AM. Intracellular Zn^{2+} content was measured by flow cytometry. (G) Cell viability recovered by BafA1 was determined by MTT assay. (H) Accumulation of LC3 lipidation and p62 by BafA1 confirmed by Western blot. (I) Western blot bands were quantified by Image J. (J) HK2 cells were transfected with GFP-LC3-RFP plasmids. The single and merged images of GFP and RFP were visualized by confocal microscopy. All data are represented as mean ± SEM. *p < 0.05, **p < 0.01, ***p < 0.001, and ****p < 0.0001.

proteolysis of poly ADP-ribose polymerase (PARP) due to inhibition of caspase 3 activity [28]. It has been proposed that one of Zn^{2+} binding sites in caspase 9 was responsible for Zn^{2+}-mediated inhibition [29]. More recently, inhibition of caspase 3, 6–8 by Zn^{2+} has been shown at nanomolar levels with Zn^{2+} binding stoichiometry [27]. Thus, the current results imply ZnO NPs may not mediate apoptotic cell death carried out by caspase cascade in HK2. Previous studies have investigated that ZnO NPs induce autophagy in various cell types. Many autophagosomes

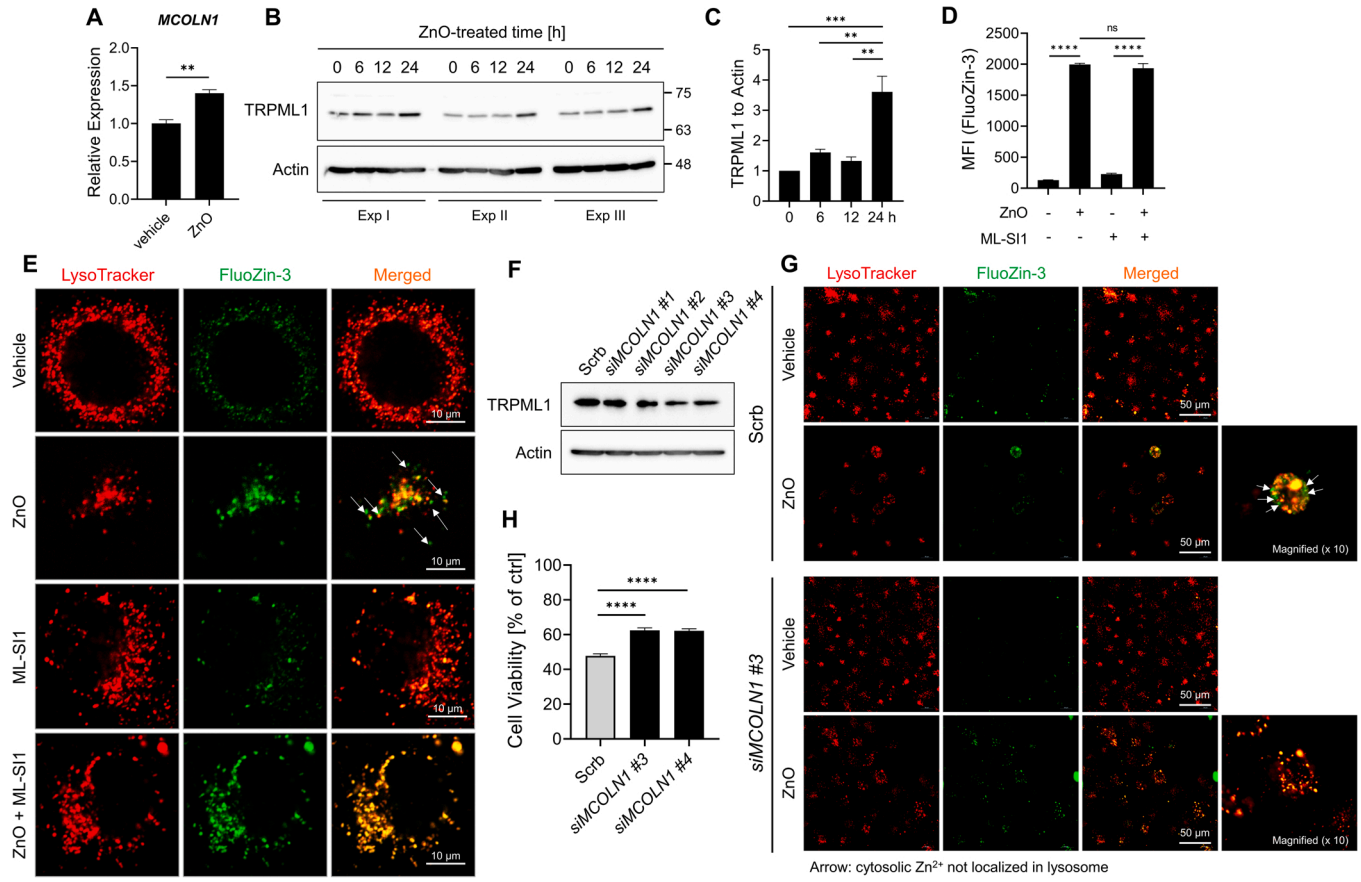

Fig. 4. ZnO NPs activate TRPML1 to release lysosomal Zn^{2+} to cytosol. (A) HK2 cells were cultured in presence of ZnO NPs for 24 h. qRT-PCR data shows MCOLN1 expression induced by ZnO NPs. (B) TRPML1 protein expression was determined by Western blot. (C) Western blot data was quantified by Image J. (D) After treating ZnO NPs and 20 μM ML-SI1 for 24 h, the cells were stained with FluoZin-3 AM. Intracellular Zn^{2+} content was measured by flow cytometry. (E) Zn^{2+} retention was visualized by confocal microscopy. Lysosomes and Zn^{2+} were detected using LysoTracker and FluoZin-3 AM, respectively. (F) Western blot data show the reduction of TRPML1 by knockdown using siRNA duplexes against MCOLN1. (G) Zn^{2+} retention after knockdown of MCOLN1 (siRNA duplex #3) was visualized by confocal microscopy. (H) HK2 cells were treated with ZnO NPs (20 μg/ml) after knockdown using siRNA duplexes #3 and #4 against MCOLN1 and negative control siRNA (scrb). Cell viability was determined by MTT assay. All data are represented as mean ± SEM. $^{**}p < 0.01$, $^{***}p < 0.001$, and $^{****}p < 0.0001$.

and autolysosomes were found in murine astrocytes exposed to ZnO NPs and level of LC3 was increased via PI3K and MAPK activation resulting from oxidative stress [30]. Acute exposure to ZnO NPs induced autophagy in primary human T cells and immortalized immune cells *in vitro* and caused immunotoxicity *in vivo* [31]. In addition, ZnO NPs triggered initiation of autophagy through lysosomal and mitochondrial dysfunction; however, autophagic flux was arrested in lung epithelial cells [32]. Our current study coincides with the fact that ZnO NPs initiate autophagy in HK2 cells as like other cell types. However, ZnO NPs-mediated cell death in HK2 cells contradict with previous investigation. As mentioned above, since excessive Zn^{2+} caused by treatment of ZnO NPs interrupted caspase activity, apoptosis was not able to occur in HK2 cells. Instead of apoptotic pathway, treatment of ZnO NPs formed autophagosome and enhanced the fusion of autophagosome and lysosome, which in turn induced cell death. Thus, we concluded ZnO NPs mediate autophagic cell death, not passing through caspase cascade due to cytosolic Zn^{2+}.

TRPML1 encoded by *MCOLN1* is a non-selective cation channel in the membrane of late endosomes and lysosomes, which is involved in regulating their functions including acidification, trafficking, membrane fusion, and autophagy [16,33,34]. Lysosomal Ca^{2+} released by the activated TRPML1 stimulates nuclear translocation of TFEB that is a key regulator of lysosomal biogenesis and autophagy [21,35,36]. Like Ca^{2+}, heavy metals including Fe^{2+} and Zn^{2+} are also permeable through TRPML1 from lysosome lumen to cytoplasm [37]. In the present study, TRPML1 expression as well as *MCOLN1* was increased in response to treatment of ZnO NPs. Although the inhibition of TRPML1 activity did not affect total level of intracellular Zn^{2+}, it allowed Zn^{2+} to be more concentrated in lysosomes than cytosol by blocking efflux of lysosomal Zn^{2+}. Based on these findings, we suggest TRPML1 activated by ZnO NPs significantly participates in regulating lysosomal Zn^{2+} efflux. A previously published paper showed that an activator of TRPML1 (ML-SA1) had evoked lysosomal Ca^{2+} release to cytosol, but Ca^{2+} and TFEB had been not required for TRPML1-mediated Zn^{2+} efflux in cancer cells [23]. Based on this paper, the effect of lysosomal Ca^{2+} release through TRPML1 could be probably ruled out on Zn^{2+}-mediated autophagic cell death in our study. The excessive level of Zn^{2+} due to ZnO NPs triggers cellular toxicity through induction of oxidative stress and ROS, which in turn elicits DNA damage and cell death [38,39]. Recently, it has been reported that the activation of TRPML1 to release lysosomal cations is directly mediated by exogenous oxidant and endogenous ROS [22]. The activation of TRPML1 causes mitochondrial damage and stimulates efflux of lysosomal Zn^{2+} in melanoma cells [23]. Enhancement of TRPML1 using specific agonists ML-SA5 and MK6–83 promotes autophagy initiation through increase of cytosolic Zn^{2+} in cancer cells [40]. Along the lines of evidence, we observed that an increase of intracellular ROS in response to ZnO NPs stimulated to generate intracellular Zn^{2+}, and scavenging ROS with NAC allowed Zn^{2+} to be localized to lysosomes. Hence, these findings imply TRPML1 can be triggered by ROS to release Zn^{2+} from lysosomes in response to ZnO NPs.

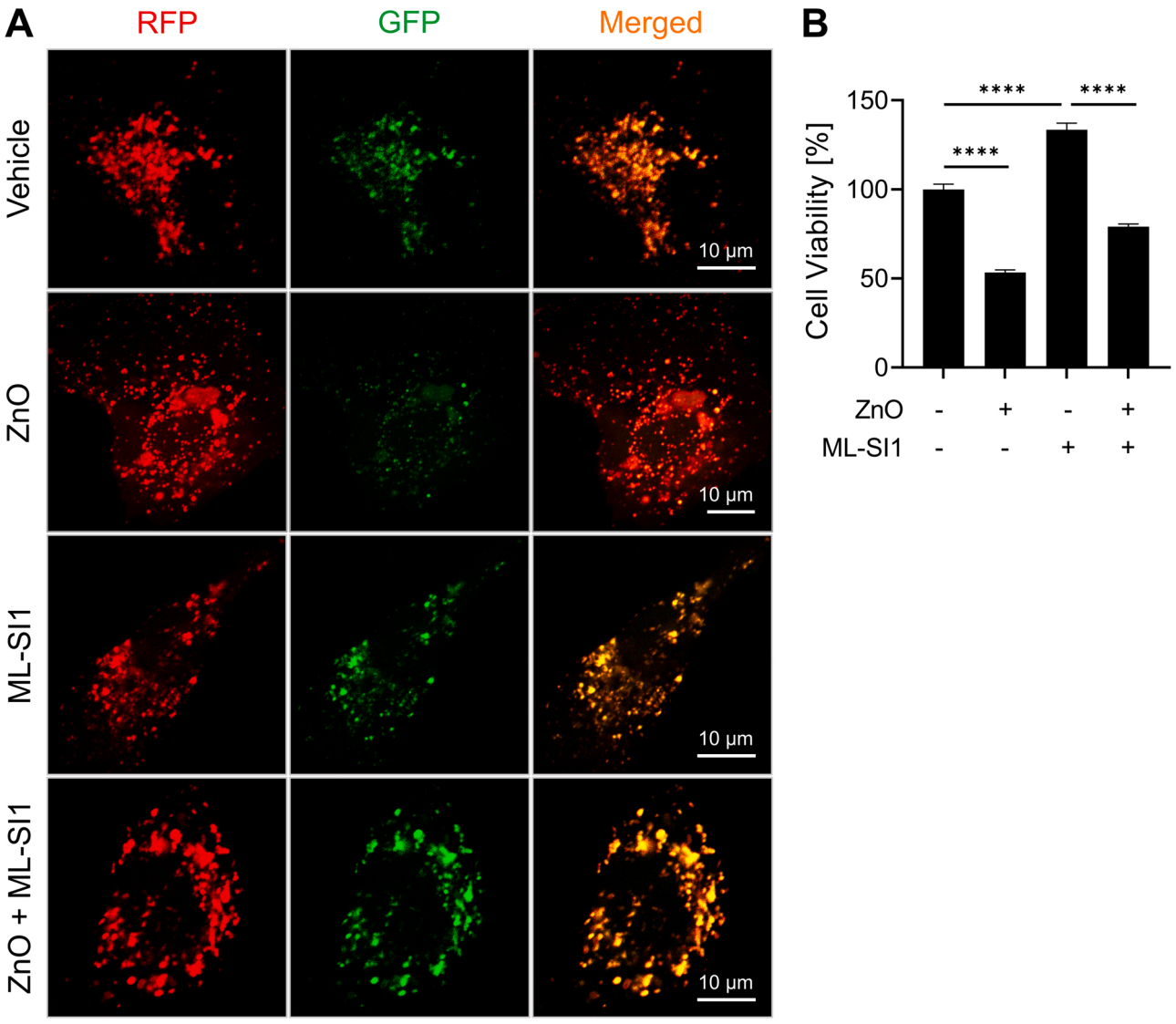

Fig. 5. TRPML1 inhibition blocks autophagic flux. (A) HK2 cells were exposed to ZnO NP for 24 h following transfected with GFP-LC3-RFP plasmids. The single and merged images of GFP and RFP were visualized by confocal microscopy. (B) Cell viability recovered by 20 μM ML-SI1 was determined using MTT assay. All data are represented as mean ± SEM. ****$p < 0.0001$.

CRediT authorship contribution statement

Boyun Kim: Conceptualization, Methodology, Software, Formal analysis, Writing – original draft, Writing – review & editing, Data curation. **Gaeun Kim**: Validation, Data curation. **Soyeon Jeon**: Methodology, Formal analysis, Investigation. **Wan-Seob Cho:** Methodology, Formal analysis, Investigation. **Hyun Pyo Jeon:** Conceptualization, Writing – original draft, Funding acquisition. **Jewon Jung:** Conceptualization, Writing – original draft, Writing – review & editing, Visualization, Resources, Supervision, Project administration, Funding acquisition.

Funding

This research was supported by Korea Basic Science Institute (National Research Facilities and Equipment Center) grant funded by the Ministry of Education [2019R1A6C1010044 and 2021R1A6C103A387], and the National Research Foundation of Korea (NRF) grant funded by the Korea government (MSIT) [2021R1F1A1050105]. H.J. was supported by the Chemical safety management specialist training program (2021) funded by Korea Chemicals Management Association (KCMA).

Declaration of Competing Interest

The authors declare that they have no known competing financial interests or personal relationships that could have appeared to influence the work reported in this paper.

Data Availability

No data was used for the research described in the article.

Appendix A. Supporting information

Supplementary data associated with this article can be found in the online version at doi:10.1016/j.toxrep.2023.04.012.

References

[1] D. Segets, J. Gradl, R.K. Taylor, V. Vassilev, W. Peukert, Analysis of optical absorbance spectra for the determination of ZnO nanoparticle size distribution, solubility, and surface energy, ACS Nano 3 (7) (2009) 1703–1710.

[2] P.K. Mishra, H. Mishra, A. Ekielski, S. Talegaonkar, B. Vaidya, Zinc oxide nanoparticles: a promising nanomaterial for biomedical applications, Drug Discov. Today 22 (12) (2017) 1825–1834.
[3] A. Czyzowska, A. Barbasz, A review: zinc oxide nanoparticles – friends or enemies? Int. J. Environ. Health Res. 32 (4) (2022) 885–901.
[4] S. Singh, Zinc oxide nanoparticles impacts: cytotoxicity, genotoxicity, developmental toxicity, and neurotoxicity, Toxicol. Mech. Methods 29 (4) (2019) 300–311.
[5] V. Sharma, P. Singh, A.K. Pandey, A. Dhawan, Induction of oxidative stress, DNA damage and apoptosis in mouse liver after sub-acute oral exposure to zinc oxide nanoparticles, Mutat. Res. 745 (1–2) (2012) 84–91.
[6] L. Xiao, C. Liu, X. Chen, Z. Yang, Zinc oxide nanoparticles induce renal toxicity through reactive oxygen species, Food Chem. Toxicol. 90 (2016) 76–83.
[7] W. Maret, The redox biology of redox-inert zinc ions, Free Radic. Biol. Med. 134 (2019) 311–326.
[8] K.M. Hambidge, N.F. Krebs, Zinc deficiency: a special challenge, J. Nutr. 137 (4) (2007) 1101–1105.
[9] A.S. Prasad, Discovery of human zinc deficiency: its impact on human health and disease, Adv. Nutr. 4 (2) (2013) 176–190.
[10] H. Tamano, Y. Koike, H. Nakada, Y. Shakushi, A. Takeda, Significance of synaptic Zn(2+) signaling in zincergic and non-zincergic synapses in the hippocampus in cognition, J. Trace Elem. Med. Biol. 38 (2016) 93–98.
[11] L. Rink, P. Gabriel, Zinc and the immune system, Proc. Nutr. Soc. 59 (4) (2000) 541–552.
[12] F.S.M. Tekie, M. Hajiramezanali, P. Geramifar, M. Raoufi, R. Dinarvand, M. Soleimani, et al., Controlling evolution of protein corona: a prosperous approach to improve chitosan-based nanoparticle biodistribution and half-life, Sci. Rep. 10 (1) (2020) 9664.
[13] Y.F. Lin, I.J. Chiu, F.Y. Cheng, Y.H. Lee, Y.J. Wang, Y.H. Hsu, et al., The role of hypoxia-inducible factor-1alpha in zinc oxide nanoparticle-induced nephrotoxicity in vitro and in vivo, Part Fibre Toxicol. 13 (1) (2016) 52.
[14] B. Halamoda Kenzaoui, C. Chapuis Bernasconi, S. Guney-Ayra, L. Juillerat-Jeanneret, Induction of oxidative stress, lysosome activation and autophagy by nanoparticles in human brain-derived endothelial cells, Biochem. J. 441 (3) (2012) 813–821.
[15] I. Kukic, J.K. Lee, J. Coblentz, S.L. Kelleher, K. Kiselyov, Zinc-dependent lysosomal enlargement in TRPML1-deficient cells involves MTF-1 transcription factor and ZnT4 (Slc30a4) transporter, Biochem. J. 451 (2) (2013) 155–163.
[16] X. Cheng, D. Shen, M. Samie, H. Xu, Mucolipins: intracellular TRPML1–3 channels, FEBS Lett. 584 (10) (2010) 2013–2021.
[17] X.P. Dong, X. Cheng, E. Mills, M. Delling, F. Wang, T. Kurz, et al., The type IV mucolipidosis-associated protein TRPML1 is an endolysosomal iron release channel, Nature 455 (7215) (2008) 992–996.
[18] H. Fares, I. Greenwald, Regulation of endocytosis by CUP-5, the Caenorhabditis elegans mucolipin-1 homolog, Nat. Genet. 28 (1) (2001) 64–68.
[19] D.L. Medina, A. Fraldi, V. Bouche, F. Annunziata, G. Mansueto, C. Spampanato, et al., Transcriptional activation of lysosomal exocytosis promotes cellular clearance, Dev. Cell 21 (3) (2011) 421–430.
[20] W. Wang, Q. Gao, M. Yang, X. Zhang, L. Yu, M. Lawas, et al., Up-regulation of lysosomal TRPML1 channels is essential for lysosomal adaptation to nutrient starvation, Proc. Natl. Acad. Sci. USA 112 (11) (2015) E1373–E1381.
[21] H. Xu, D. Ren, Lysosomal physiology, Annu. Rev. Physiol. 77 (2015) 57–80.
[22] X. Zhang, X. Cheng, L. Yu, J. Yang, R. Calvo, S. Patnaik, et al., MCOLN1 is a ROS sensor in lysosomes that regulates autophagy, Nat. Commun. 7 (2016) 12109.
[23] W. Du, M. Gu, M. Hu, P. Pinchi, W. Chen, M. Ryan, et al., Lysosomal Zn(2+) release triggers rapid, mitochondria-mediated, non-apoptotic cell death in metastatic melanoma, Cell Rep. 37 (3) (2021), 109848.
[24] A. Lopez, A. Fleming, D.C. Rubinsztein, Seeing is believing: methods to monitor vertebrate autophagy in vivo, Open Biol. 8 (10) (2018).
[25] A. Manke, L. Wang, Y. Rojanasakul, Mechanisms of nanoparticle-induced oxidative stress and toxicity, BioMed Res. Int. 2013 (2013), 942916.
[26] X. Qin, J. Zhang, B. Wang, G. Xu, Z. Zou, LAMP-2 mediates oxidative stress-dependent cell death in Zn(2+)-treated lung epithelium cells, Biochem. Biophys. Res. Commun. 488 (1) (2017) 177–181.
[27] S.J. Eron, D.J. MacPherson, K.B. Dagbay, J.A. Hardy, Multiple mechanisms of zinc-mediated inhibition for the apoptotic caspases-3, -6, -7, and -8, ACS Chem. Biol. 13 (5) (2018) 1279–1290.
[28] D.K. Perry, M.J. Smyth, H.R. Stennicke, G.S. Salvesen, P. Duriez, G.G. Poirier, et al., Zinc is a potent inhibitor of the apoptotic protease, caspase-3. A novel target for zinc in the inhibition of apoptosis, J. Biol. Chem. 272 (30) (1997) 18530–18533.
[29] K.L. Huber, J.A. Hardy, Mechanism of zinc-mediated inhibition of caspase-9, Protein Sci. 21 (7) (2012) 1056–1065.
[30] W.J. Song, M.S. Jeong, D.M. Choi, K.N. Kim, M.B. Wie, Zinc oxide nanoparticles induce autophagy and apoptosis via oxidative injury and pro-inflammatory cytokines in primary astrocyte cultures, Nanomaterials (7) (2019) 9.
[31] B.M. Johnson, J.A. Fraietta, D.T. Gracias, J.L. Hope, C.J. Stairiker, P.R. Patel, et al., Acute exposure to ZnO nanoparticles induces autophagic immune cell death, Nanotoxicology 9 (6) (2015) 737–748.
[32] J. Zhang, X. Qin, B. Wang, G. Xu, Z. Qin, J. Wang, et al., Zinc oxide nanoparticles harness autophagy to induce cell death in lung epithelial cells, Cell Death Dis. 8 (7) (2017), e2954.
[33] S. Vergarajauregui, P.S. Connelly, M.P. Daniels, R. Puertollano, Autophagic dysfunction in mucolipidosis type IV patients, Hum. Mol. Genet. 17 (17) (2008) 2723–2737.
[34] K. Venkatachalam, C.O. Wong, M.X. Zhu, The role of TRPMLs in endolysosomal trafficking and function, Cell Calcium 58 (1) (2015) 48–56.
[35] C. Sagne, B. Gasnier, Molecular physiology and pathophysiology of lysosomal membrane transporters, J. Inherit. Metab. Dis. 31 (2) (2008) 258–266.
[36] D.L. Medina, S. Di Paola, I. Peluso, A. Armani, D. De Stefani, R. Venditti, et al., Lysosomal calcium signalling regulates autophagy through calcineurin and TFEB, Nat. Cell Biol. 17 (3) (2015) 288–299.
[37] W. Wang, X. Zhang, Q. Gao, H. Xu, TRPML1: an ion channel in the lysosome, Handb. Exp. Pharm. 222 (2014) 631–645.
[38] R.S. Kumaran, Y.K. Choi, V. Singh, K.J. Kim, H.J. Kim, Cytotoxic effects of ZnO nanoparticles on the expression of ROS-responsive genes in the human cell lines, J. Nanosci. Nanotechnol. 16 (1) (2016) 210–218.
[39] S.H. Jeong, H.J. Kim, H.J. Ryu, W.I. Ryu, Y.H. Park, H.C. Bae, et al., ZnO nanoparticles induce TNF-alpha expression via ROS-ERK-Egr-1 pathway in human keratinocytes, J. Dermatol. Sci. 72 (3) (2013) 263–273.
[40] J. Qi, Y. Xing, Y. Liu, M.M. Wang, X. Wei, Z. Sui, et al., MCOLN1/TRPML1 finely controls oncogenic autophagy in cancer by mediating zinc influx, Autophagy 17 (12) (2021) 4401–4422.